

1 Original article

2 **Root cortical aerenchyma inhibits radial nutrient transport in maize (*Zea mays* L.)**

3 Bo Hu<sup>1,2</sup>, Amelia Henry<sup>3</sup>, Kathleen M. Brown<sup>1,3</sup>, and Jonathan P. Lynch<sup>1,3\*</sup>

4 <sup>1</sup>Department of Plant Science, The Pennsylvania State University, University Park, PA 16802  
5 USA

6 <sup>2</sup> Agriculture Department, Inner Mongolia Agriculture University, Hohhot, P.R.China

7 <sup>3</sup>Intercollege Program in Plant Biology, The Pennsylvania State University, University Park,  
8 PA 16802 USA

9 Running title: Root cortical aerenchyma inhibits radial nutrient transport in maize

10

11 \*Corresponding author ([jpl4@psu.edu](mailto:jpl4@psu.edu); Tel: +1-814-863-2256; Fax: +1-814-863-6139)

12

13

14 **Abstract**

15 • *Background and Aims* Formation of root cortical aerenchyma (RCA) can be induced by  
16 nutrient deficiency. In species adapted to aerobic soil conditions, this response is adaptive by  
17 reducing root maintenance requirements, thereby permitting greater soil exploration. One  
18 trade-off of RCA formation may be reduced radial transport of nutrients due to reduction in  
19 living cortical tissue. To test this hypothesis, radial nutrient transport in intact roots of maize  
20 (*Zea mays* L.) was investigated in two radiolabeling experiments employing genotypes with  
21 contrasting RCA.

22 • *Methods* In the first experiment, time-course dynamics of phosphate loading into the xylem  
23 were measured from excised nodal roots that varied in RCA formation. In the second  
24 experiment, uptake of phosphate, calcium and sulfate was measured in seminal roots of intact  
25 young plants in which variation in RCA was induced by treatments altering ethylene action  
26 or genetic differences.

27 • *Key Results* In each of three paired genotype comparisons, the rate of phosphate exudation  
28 of high RCA genotypes was significantly less than that of low RCA genotypes. In the second  
29 experiment, radial nutrient transport of phosphate and calcium was negatively correlated with  
30 the extent of RCA for some genotypes.

31 • *Conclusions* Our results support the hypothesis that RCA can reduce radial transport of  
32 some nutrients in some genotypes, which could be an important trade-off of this trait.

33 **Key words**

34 Aerenchyma, radial transport, root, phosphorus, sulfur, calcium, *Zea mays* L.

35

36

## 37 INTRODUCTION

38 Root cortical aerenchyma (RCA) in maize is formed by programmed cell death of cortical  
39 cells, leaving air-filled lacunae (Esau 1977). RCA is induced by a variety of stimuli including  
40 hypoxia, nutrient deficiency, mechanical impedance, and drought (Drew et al. 1980, 2000;  
41 He et al. 1996; Bouranis et al. 2003; Zhu et al. 2010). We hypothesized that RCA may be an  
42 adaptive response to nutrient stress by reducing the metabolic cost of soil exploration (Lynch  
43 and Brown 1998). In support of this hypothesis, Fan et al. (2003) observed a 70% decrease in  
44 respiration of maize (*Zea mays* L.) aerenchymatous roots compared to non-aerenchymatous  
45 roots, and showed that RCA formation was negatively correlated with respiration and tissue  
46 phosphorus content when RCA formation was manipulated by genetics, phosphorus  
47 availability, or ethylene. Similarly, respiration rates were lower in seminal roots of maize  
48 genotypes that produced large amounts of RCA under drought stress, and this was associated  
49 with greater rooting depth, improved leaf water status, shoot growth, and yield (Zhu et al.  
50 2010). Simulations with the structural-functional model, *SimRoot*, predicted that RCA would  
51 increase growth under low phosphorus, potassium, or nitrogen stress by remobilizing  
52 nutrients from the root cortex and reducing root respiration (Postma and Lynch 2010, 2011).

53 Tradeoffs for RCA formation are not understood, but the presence of genetic variation within  
54 maize for this trait suggests that RCA formation confers both benefits and costs. A study of  
55 the effect of RCA on root mechanical strength, measured as resistance to radial compression,  
56 showed that species with multiseriate rings in the outer cortex, including maize, were not  
57 weakened by the presence of flooding-induced RCA, while species lacking the multiseriate  
58 rings collapsed more readily (Striker et al. 2007). RCA formed under phosphorus deficiency  
59 contributed to reduced radial hydraulic conductivity in maize roots (Fan et al. 2007). An  
60 additional possible trade-off of RCA formation may be reduced radial transport of nutrients  
61 across the cortex, caused by longer path length and reduced cross sectional area of both  
62 apoplastic and symplastic pathways. This study tests this hypothesis by examining the effects  
63 of RCA on radial transport of phosphate, calcium, and sulfate in maize roots. We used natural  
64 genetic variation as well as ethylene and 1-MCP (1-methylcyclopropene) treatments to  
65 produce plants with varying RCA. We hypothesized that RCA would decrease radial  
66 transport of these nutrients.

67

## 68 MATERIALS AND METHODS

69 Two sets of experiments were conducted using radiolabeling to measure the effects of RCA  
70 on radial nutrient transport; 1) a time-course study using excised roots (experiment 1), and 2)  
71 whole plant studies on nutrient uptake (experiment 2). In experiment 1, six RILs  
72 (Recombinant Inbred Lines) with contrasting RCA were used and <sup>32</sup>P transport and exudation  
73 were measured in a short segment of an excised nodal root. In experiment 2, a range of RCA  
74 expression was generated by making use of genetic variation among three RILs and  
75 treatments with 1-MCP and ethylene. Segments of intact seminal roots were exposed to <sup>45</sup>Ca,  
76 <sup>32</sup>P, or <sup>35</sup>S and radioactivity was measured in shoots and nutrient solution to assess nutrient  
77 transport.

### 78 *Plant materials and culture*

79 Recombinant inbred lines (RIL 15, RIL 345, RIL 360, RIL 369, RIL 61, RIL 321 in

80 experiment 1 and RIL 39, RIL 76, and RIL 364 in experiment 2) of maize (*Zea mays* L.) from  
81 the IBM (Intermated B73×Mo17) population (USDA/ARS Maize Genetics Cooperation  
82 Stock Center, Urbana IL) were selected for this study based on contrasting RCA formation in  
83 screening studies. Plant growth conditions were similar in the two experiments. Seeds were  
84 surface sterilized in 50% bleach (3% NaOCl), imbibed in a Benomyl solution (DuPont,  
85 Wilmington DE; 5 g L<sup>-1</sup> for 3h in experiment 1; 8 g L<sup>-1</sup> for 1.5h in experiment 2), then  
86 transferred to germination paper (76 wt., Anchor Paper, St. Paul MN) where they were rolled  
87 up and maintained in covered beakers (5 L in experiment 1; 1 L in experiment 2) containing  
88 CaSO<sub>4</sub> (1 L of 0.5 mM in experiment 1; 150 ml of 0.25 mM in experiment 2) and Benomyl  
89 (2.5 g L<sup>-1</sup> in experiment 1; 4 g L<sup>-1</sup> in experiment 2) at 28 °C (4 d in experiment 1; 6 d in  
90 experiment 2) in a dark chamber. In experiment 1, germinated seedlings in rolls were then  
91 placed under a fluorescent light (~45 μmol m<sup>-2</sup> s<sup>-1</sup>) for 1d before transplanting to aerated  
92 solution culture. Seedlings (12 per container in experiment 1; 24 per container in experiment  
93 2) were transferred to open-cell foam plugs suspended above solution culture tanks (30 L in  
94 experiment 1; 100 L in experiment 2) and grown in a greenhouse at The Pennsylvania State  
95 University, USA (40° 47' N, 77° 51' W). In experiment 1, plants were grown for 12 d during  
96 the month of July when the average temperature was 33°, average humidity was 45%, and  
97 mid-day solar radiation levels averaged 720 μmol m<sup>-2</sup> s<sup>-1</sup>. In experiment 2, plants were grown  
98 for seven to eight days in the month of March, when temperatures averaged 29 °C and mid-  
99 day solar radiation levels averaged 400 μmol m<sup>-2</sup> s<sup>-1</sup>. Ambient light was supplemented with  
100 metal halide lamps (~150 μmol m<sup>-2</sup> s<sup>-1</sup>; 16 h photoperiod). The nutrient solution (pH = 4.5)  
101 contained 3 mM KNO<sub>3</sub>, 2 mM Ca(NO<sub>3</sub>)<sub>2</sub>, 0.5 mM MgSO<sub>4</sub>, 0.5 mM (NH<sub>4</sub>)<sub>2</sub>SO<sub>4</sub>, 0.5 mM  
102 NH<sub>4</sub>H<sub>2</sub>PO<sub>4</sub>, 25 μM H<sub>3</sub>BO<sub>3</sub>, 0.5 μM CuSO<sub>4</sub>, 50 μM Fe-DTPA, 2 μM MnSO<sub>4</sub>, 0.5 μM  
103 (NH<sub>4</sub>)<sub>6</sub>Mo<sub>7</sub>O<sub>24</sub>, 2 μM ZnSO<sub>4</sub>, 50 μM KCl, and 50 μM FeNH<sub>4</sub>SO<sub>4</sub>. In experiment 1, the pH of  
104 the nutrient solution was adjusted every 2 d to 5.5 with KOH, and the nutrient solution was  
105 replaced entirely every 7 d.

#### 106 *Ethylene and 1-MCP treatments*

107 Root treatments to manipulate RCA production in experiment 2 included a control (air), root-  
108 zone ethylene application, and root-zone 1-MCP (1-methylcyclopropene) application, applied  
109 continuously beginning at seedling transfer to solution culture. Ethylene promotes RCA  
110 formation (Evans 2003), and 1-MCP reduces RCA formation (Fan et al. 2003) by inhibiting  
111 ethylene action. Solution culture tanks in the control treatment were bubbled at 30 ml min<sup>-1</sup>  
112 with ambient air. In the ethylene treatment, compressed ethylene (1 μl L<sup>-1</sup> in air, as used by  
113 Gunawardena *et al.* (2001) was bubbled through solution culture tanks at 30 ml min<sup>-1</sup>.  
114 Ethylene concentrations in the headspace of solution culture tanks were measured  
115 periodically by gas chromatography (Hewlett-Packard 6890) and averaged 0.56 ± 0.06 μl L<sup>-1</sup>.  
116 For the 1-MCP treatment, 1-methylcyclopropene (3.8 % active ingredient, Rohm and Haas,  
117 Philadelphia PA) was volatilized by dissolving 0.17 g in 5 ml water in a glass scintillation  
118 vial, and then transferred quickly into a 2-L sidearm flask. An open-cell foam plug was used  
119 to enclose the mouth of the flask, and the headspace containing 1-MCP gas was bubbled  
120 through 3 100-L tanks at a rate of 30 ml min<sup>-1</sup> in each tank to achieve a 1-MCP concentration  
121 of 7.7 μl L<sup>-1</sup> solution, assuming all 1-MCP dissolved in solution. The air pump ran  
122 continuously, and the 1-MCP was replenished daily into the sidearm flask.

#### 123 *Radionuclide treatments*

#### 124 *Experiment 1: <sup>32</sup>P transport dynamics in excised root segments*

125 Experiment 1 was performed to measure movement of  $^{32}\text{P}$  in excised root segments. Pairs of  
126 RILs were selected for simultaneous testing based on contrasting RCA phenotypes in  
127 previous screening studies. Plants were transferred to a laboratory adjacent to the greenhouse.  
128 The apical 8 cm of a first-whorl nodal root was excised and installed in a modified Pitman  
129 chamber (Fig.1A) (Lynch and Läuchli 1984) permitting treatment of a known length of root  
130 (in this case 7.4 mm) with radionuclide. A 10 mm segment of root extended from the 1-ml  
131 treatment compartment to the 0.5 ml receiver compartment (Fig. 1A). Silicon grease (Dow  
132 Corning, Midland MI) was used to isolate the compartments from each other. A solution with  
133 0.5 mM  $\text{CaSO}_4$ , 0.5 mM  $\text{KNO}_3$  and 0.05 mM  $\text{KH}_2\text{PO}_4$  at pH 6.0 was added to the treatment  
134 compartment, receiver compartment, and the space around the root tip. The entire assembly  
135 with the root tip was sealed with silicon grease and placed in a temperature-controlled water  
136 bath at 25°.

137 Sixty minutes after excision, the solution in the treatment compartment was replaced with  
138 fresh nutrient solution containing approximately 10  $\mu\text{Ci}$   $^{32}\text{PO}_4$ . The solution in the receiver  
139 compartment was mixed and then sampled 5 times at 15 min intervals by withdrawing 400  $\mu\text{l}$   
140 of solution. When sampling was complete, the remaining 100 $\mu\text{l}$  of exudation solution in the  
141 receiver compartment was removed and discarded, and then the receiver compartment was  
142 refilled with 0.5 ml of nutrient solution without  $^{32}\text{P}$ . The solution in the treatment  
143 compartment was replaced with 0.05 % toluidine blue for 4 min to mark the root region  
144 exposed to  $^{32}\text{P}$ . Leakage between compartments could be easily detected by movement of the  
145 toluidine blue to the receiver or leakage check chambers. Data from chambers showing any  
146 sign of compartment leakage (detected by blue dye) were discarded.

147 Due to constraints of the experiment, it was not possible to measure all six genotypes on a  
148 given day. Therefore genotypes were paired for contrast in RCA abundance, one high and  
149 one low per pair. Roots from two contrasting RCA genotypes were simultaneously exposed  
150 to  $^{32}\text{P}$  in separate chambers. One root was placed in each chamber and 4 replicates of each  
151 genotype were measured sequentially in each experiment. Each experiment was repeated  
152 twice for a total of 8 replicates for each genotype. Root segments from the treatment  
153 compartment, now dyed blue, were excised and stored in 70 % ethanol for anatomical  
154 analysis. To assess  $^{32}\text{P}$  accumulation within the root, the 10 mm segment extending from the  
155 treatment compartment to the receiver compartment (Fig. 1A) was ashed for 20 h at 500°.  
156 Acropetal movement of  $^{32}\text{P}$  was checked by sampling the leakage check compartment, the  
157 nutrient solution bathing the root tip, and ashed root tip samples, and no radioactivity was  
158 found. Samples were suspended in a gelling scintillation solvent (ScintiSafe Gel Cocktail,  
159 Fisher Scientific) and analyzed by liquid scintillation spectroscopy (Packard Tri-Carb 1500,  
160 Packard Instruments, Meriden, CT, USA). The counts per million (cpm) for  $^{32}\text{P}$  exudation  
161 into the receiver compartment and the cpm for  $^{32}\text{P}$  within the 10 mm root section extending  
162 from the treatment compartment to the receiving chamber were added for calculation of  $^{32}\text{P}$   
163 influx, i.e. these values include all  $^{32}\text{P}$  that was taken up and transported into the treatment  
164 compartment.  $^{32}\text{P}$  exudation refers to only the  $^{32}\text{P}$  that moved into the receiver compartment  
165 solution.

#### 166 *Experiment 2: Radial transport of phosphate, calcium, and sulfate by roots of whole plants*

167 Experiment 2 was conducted to evaluate radial nutrient transport in whole plants, when  
168 radiolabel was applied to small seminal root segments of varying RCA levels. Seedlings were  
169 transferred to a laboratory adjacent to the greenhouse in 100-ml cups containing nutrient

170 solution from the solution culture tanks, covering the entire root zone (Fig. 1B). Radionuclide  
171 application chambers were constructed from a 500  $\mu$ l polypropylene tube (Axygen Scientific,  
172 Union City CA) with two opposing 3 mm diameter holes in the sidewalls, rested on the edge  
173 of the cup by the tube lid. One seminal root from each plant was threaded through the holes  
174 in the tube and sealed with silicon grease isolating a 6 mm length of root (the inner diameter  
175 of the tube) for exposure to radionuclides. Exposed root regions were at the basipetal end of  
176 the seminal root, 10-50 mm from the hypocotyl, and remained attached to the intact plant.  
177 The basipetal region of seminal roots was chosen for this experiment to maximize RCA  
178 variation, since in preliminary studies showed little RCA formation in sections greater than  
179 50 mm from the hypocotyl. This location also allowed for consistency in distance from the  
180 hypocotyl, which would have been greatly affected by root length if apical parts had been  
181 used. Nutrient solution (500  $\mu$ l) without the element to be applied as radionuclide was added  
182 to the radionuclide application chamber for the short time (about 30 min) between sealing the  
183 root and adding the radionuclide in order to keep the root moist and be able to accurately  
184 calculate specific activities once the radionuclide was added.

185  
186 The isolated root segments were exposed to 10  $\mu$ Ci  $^{32}$ P-phosphate,  $^{45}$ Ca, or  $^{35}$ S-sulfate (MP  
187 Biomedicals, Solon, OH, USA) in 50  $\mu$ l complete nutrient solution (described above for  
188 solution culture in the greenhouse). Plants were incubated under a metal halide lamp  
189 providing 150  $\mu$ mol photons  $\text{m}^{-2} \text{s}^{-1}$ , with the root zone covered with aluminum foil and  
190 maintained at 25  $^{\circ}$ C by a circulating water bath surrounding the 100 ml cups. Plants from one  
191 full replicate (three treatments for three genotypes) were exposed to a single radionuclide at  
192 the same time, and six replicates were used for each radionuclide for a total of 162 plants.  
193 After 30 min, shoots were excised, transferred to pre-weighed 20 ml scintillation vials, dried  
194 at 60  $^{\circ}$ C, and weighed. Solution from the outer cup was sampled (500  $\mu$ l) and dissolved in 10  
195 ml scintillation cocktail (ScintiSafe Gel Cocktail for  $^{32}$ P and  $^{45}$ Ca treatments, ScintiSafe  
196 Econo Cocktail for  $^{35}$ S treatments, Fisher Scientific) to check for radionuclide leaks from the  
197 application chamber. Samples were discarded if leaks were observed. Root regions to which  
198 radionuclide was applied were excised and stored in 25 % ethanol for later anatomical  
199 analysis. The remaining root system from each plant was then transferred to a 20 ml  
200 scintillation vial, dried at 60  $^{\circ}$ C, and weighed.

201  
202 Radionuclide content in the entire shoot of each plant was determined in the  $^{32}$ P and  $^{45}$ Ca  
203 treatments from ashed tissue (20 hours at 500  $^{\circ}$ C) suspended in scintillation gel (ScintiSafe  
204 Gel Cocktail, Fisher Scientific) using a liquid scintillation spectrometer (Packard Tri-Carb  
205 1500). Radionuclide content in shoots from the  $^{35}$ S treatment was determined according to  
206 (Naeve and Shibles 2005). Dried shoots were pulverized in a plastic scintillation vial with a  
207 methacrylate ball in a Mixer Mill 8000 (Spex, Inc.). Tissue was decolorized by adding 1-2 ml  
208 6% NaOCl and incubating 2 h at 65  $^{\circ}$ C with vials tightly capped. Tissue was then suspended  
209 in scintillation cocktail (ScintiSafe Econo Cocktail, Fisher Scientific) and counted on a liquid  
210 scintillation spectrometer with quench correction by transformed spectral index of the  
211 external standard.

### 212 *Morphological and anatomical characterization*

213 The number of lateral roots was determined in each root segment to which radionuclide was  
214 applied, and root segments from the radionuclide-treated areas were hand-sectioned under a  
215 dissecting microscope (Nikon SMZ-U). Images of cross-sections (3 per sample in experiment  
216 1; 5 in experiment 2) were acquired on a compound microscope (Nikon Diaphot; 40x or 100x

217 magnification). Images were analyzed for total root cross-sectional area (RXSA), stele area  
218 (SA), and % root cortical aerenchyma area in the cortex (%RCA) using *RootScan* (Burton et  
219 al. 2012) in experiment 1 and in GIMP v. 2.5 based on pixel number in experiment 2. Root  
220 hairs were present in some samples and were rated in experiment 2 on a scale of 0-5, where 5  
221 is highest, considering both number and length. Root hairs were very scarce in experiment 1  
222 and were not included in the analyses. Surface area of the exposed root segment was  
223 estimated as the surface area of a cylinder, with the length determined by toluidine blue  
224 staining, and the radius calculated from the cross sectional area. In experiment 1, any lateral  
225 roots that were present were just emerging, so surface area of each lateral root was estimated  
226 as the lateral surface area of a cone, with an estimated (based on visual observation) height of  
227 1 mm and radius of 0.5 mm, for a total of  $<1 \text{ mm}^2$  per lateral root. The additional surface area  
228 contributed by lateral roots was found to be negligible (the maximum number of lateral roots  
229 would add less than 3% to the surface area), so these were ignored in P efflux calculations.  
230 Lateral roots were more prevalent in experiment 2 and were quantified by counting the  
231 number of lateral roots per segment of radionuclide-treated root.

232  
233 Data were analyzed by linear regression, multiple regression, and ANOVA using SAS 9.0  
234 (SAS Institute Inc., Cary, NC, USA) in the first set of experiments and using SPSS v. 11  
235 (SPSS Inc., 2005) in the second set of experiments. Data from each genotype were checked  
236 for homogeneity of variance.

## 237 RESULTS

### 238 *Experiment 1: $^{32}\text{P}$ transport dynamics in excised root segments*

239 Genetic variation among recombinant inbred lines was observed for root anatomy in the  $^{32}\text{P}$   
240 application zone (Table 1, Fig. 2). Root cross-sectional area (RXSA) and stele area (SA) were  
241 correlated ( $r^2=0.6826$ ), but the other variables including %RCA and lateral root number  
242 (LRN) were independent of each other.

### 243 *Phosphate uptake & exudation*

244 Phosphate uptake rates varied nearly 30-fold among genotypes (Table 1). Since there was  
245 genetic variation in root diameter, which would influence the surface area from which  
246 phosphate could be taken up, uptake rates were calculated on both length and surface area  
247 bases, with similar results. Coefficients of variation for phosphate influx ( $\text{pm mm}^{-2} \text{ h}^{-1}$ )  
248 averaged 0.64. Multiple regressions showed that %RCA ( $P<0.0001$ ) and LRN ( $P=0.0024$ )  
249 had significant effects on phosphate uptake, while RXSA and SA did not, despite genetic  
250 variation for these traits. There was a significant negative correlation between phosphate  
251 uptake and percentage of RCA ( $P<0.001$ , Fig. 3). A positive relationship was observed  
252 between phosphate uptake and lateral root number ( $r^2 = 0.39$ ,  $P<0.001$ ). Lateral roots did not  
253 exceed 1 mm in length. We estimated the surface area of segments bearing lateral roots using  
254 the root cross-sectional area, the segment length, the number of lateral roots, and the lateral  
255 root surface area (see Materials and Methods), and found that the small lateral roots that were  
256 present would cause less than 3% increase in surface area. Therefore the effects of lateral  
257 roots on phosphate uptake in experiment 1 were not due to the increased surface area. Lateral  
258 roots were particularly abundant on RIL 321 (5-9 lateral roots) but were also present on root  
259 samples of the other genotypes (0-3 lateral roots). If RIL 321 was omitted from the analysis,  
260 there was no relationship between P uptake and lateral root number (data not shown).

261 The time course of  $^{32}\text{P}$  exudation into the receiver chamber showed that phosphate exudation  
262 by the low RCA genotypes RIL 321, RIL 61, and RIL 369 was markedly greater than that of  
263 the high RCA genotypes RIL 360, RIL 345, and RIL 15 (Fig. 4). There was a delay of 15-30  
264 min before phosphate exudation was detected. The highest rate of exudation occurred in  
265 genotype RIL 321, which had moderate RCA and high lateral root number (Table 1, Fig. 4).  
266 Even when only the paired comparison for which both genotypes had low lateral root number  
267 is considered (RIL 61 vs RIL 345), the higher RCA genotype, RIL 345, had a slower rate of  
268  $^{32}\text{P}$  exudation.

269 *Experiment 2: Radial transport of phosphate, calcium, and sulfate by roots of whole plants*

270 *Plant growth and root traits*

271 Genetic variation for several growth attributes was observed in the control treatment (Table  
272 2). RIL 39 had the smallest dry plant mass ( $P=0.027$ ), the greatest level of RCA formation  
273 ( $P=0.014$ ), and the lowest rating for root hair growth ( $P=0.017$ ). RIL 76 had the greatest dry  
274 plant mass ( $P=0.027$ ), greatest RXSA ( $P<0.001$ ), greatest stele area (SA, as percent of root  
275 cross-sectional area;  $P=0.086$ ), and greatest number of lateral roots (LRN) in the root  
276 segment sampled ( $P<0.001$ ). Trends in plant mass reflected seed mass (g) for each genotype,  
277 which was  $0.202 \pm 0.004$  for RIL 39,  $0.315 \pm 0.005$  for RIL 76, and  $0.267 \pm 0.01$  for RIL  
278 364. Root to shoot ratio averaged  $1.20 \pm 0.06$  and did not differ among genotypes or  
279 treatments. In general, roots appeared to be more mature in experiment 2 compared to  
280 experiment 1.

281  
282 The response to ethylene and 1-MCP treatments varied with genotype (Table 2). In RIL 39,  
283 the lowest RXSA ( $P=0.005$ ) and the highest %SA ( $P<0.001$ ) were observed in the 1-MCP  
284 treatment. Treatments did not affect RCA formation in RIL 39. In RIL 76, roots in the 1-  
285 MCP treatment had significantly less RCA formation than in the ethylene treatment  
286 ( $P=0.043$ ) and both 1-MCP and ethylene reduced lateral root number ( $P=0.012$ ). RIL 364  
287 roots treated with 1-MCP had less RCA than ethylene treated roots, but this effect was  
288 significant only in roots with RXSA greater than  $1.5 \text{ mm}^2$ . Visual observations of whole root  
289 systems indicated that the 1-MCP treatment caused a lengthening of lateral roots in general.  
290 No relationship between treatment and root hair formation was observed, perhaps because  
291 root hairs formed on these segments of the roots before the seedlings were exposed to  
292 ethylene or 1-MCP.

293  
294 The combination of different genotypes and treatments yielded a wide variation in abundance  
295 of RCA (Fig. 2), ranging from 1.31% for the 1-MCP treatment of RIL 76 to 11.34 % for the  
296 1-MCP treatment of RIL 39. Coefficients of variation for percent RCA ranged from 0.48 in  
297 the 1-MCP treatment of RIL 39 to 1.91 in the 1-MCP treatment of RIL 76. The treatments  
298 affected other anatomical traits in addition to RCA, e.g. 1-MCP had a tendency to reduce  
299 RXSA and increase the proportion of stele area, but this was only significant in RIL 39. The  
300 coefficient of variation (CV) among the five sub-replicate cross-section images in almost all  
301 exposed root regions was  $<1$  for %RCA, RXSA, and %SA. No relationship was observed  
302 between plant mass and RCA in the 6-mm sampled root segments.

303  
304 *Nutrient transport*

305 Over the 30 min uptake experiments, an average of  $0.036 \pm 0.008$  nmol calcium,  $4.31 \pm 0.49$   
306 nmol phosphate, and  $20.4 \pm 2.12$  nmol sulfate was taken up by the 6-mm root segment to



307 which radionuclide was applied and transported to the shoot. Coefficients of variation for  
308 nutrient uptake were high, with values of 2.27 for calcium, 1.12 for phosphate, and 1.08 for  
309 sulfate (average CV for the study =  $1.49 \pm 0.39$ ).

310

311 When compared over all genotypes and treatments applied for each nutrient studied in  
312 experiment 2, no significant effect of RCA on radial nutrient transport was observed.  
313 However, a direct relationship was observed between nutrient transport and RCA in certain  
314 genotype and nutrient combinations (Fig. 5). For statistical analysis, a variable for classes of  
315 RXSA was created by grouping roots of  $< 0.5 \text{ mm}^2$  (far below the average area of  $1.6 \text{ mm}^2$   
316 and about 4 % of all samples),  $0.5 - 1.5 \text{ mm}^2$  (43% of all samples), and  $> 1.5 \text{ mm}^2$  (53% of  
317 all samples). Calcium transport was negatively related to RCA in RIL 76 ( $r^2=0.337$ ,  $P=0.029$ ;  
318 Fig. 5A), and also in roots with a cross-section area  $>1.5 \text{ mm}^2$  from all genotypes and  
319 treatments ( $r^2=0.124$ ,  $P=0.092$ ). Phosphate transport was negatively correlated with RCA in  
320 RIL 364 ( $r^2=0.388$ ,  $P=0.017$ ; Fig. 5B), and also in roots with a cross-section area between 0.5  
321 and  $1.5 \text{ mm}^2$  ( $r^2=0.292$ ,  $P=0.046$ ). No direct relationship between sulfate transport and RCA  
322 was observed. Other root attributes were also related to radial nutrient transport (Table 3).

323

324 Radionuclide content of a 500  $\mu\text{l}$  sample from the cup solution surrounding the main root  
325 system averaged  $16 \pm 0.4 \text{ nCi}$  for  $^{35}\text{Ca}$ ,  $25 \pm 0.5 \text{ nCi}$  for  $^{32}\text{P}$ , and  $1.18 \pm 0.03 \mu\text{Ci}$  for  $^{45}\text{S}$ .  
326 Nutrient transport was correlated with radionuclide content of the cup solution sample only  
327 for sulfate ( $r^2 = 0.096$ ,  $p = 0.022$ ).

328

## 329 DISCUSSION

330 Root cortical aerenchyma formation reduced uptake rates of phosphate in 14-16 day-old  
331 excised roots and whole maize plants, and negative trends were observed between RCA  
332 formation and uptake of sulfate and calcium in whole plants. Although large variability in  
333 nutrient transport was observed, which was likely due to variation in RCA as well as other  
334 root attributes (see Table 3), it was notable that no positive correlations between RCA  
335 formation and nutrient transport were observed.

336 Of the three nutrient ions tested, phosphate showed the most significant reduction in uptake,  
337 though calcium and sulfate uptake also tended to decline with increasing RCA (Fig. 5).  
338 Radial nutrient transport across the cortex involves both the apoplast and symplast, and  
339 nutrient ions can enter the symplastic pathway via all cell types outside the endodermis  
340 (Tester and Leigh 2001). Sulfate and phosphate share comparable internal transport  
341 pathways, predominantly through the symplast, since they are similar in size and charge.  
342 Formation of RCA could reduce nutrient transport into the symplast by reducing the number  
343 and surface area of living cells between the epidermis and stele. Apoplastic radial pathways  
344 through the cortex would also be more tortuous, with fewer intercellular routes. On the other  
345 hand, if some aerenchyma lacunae are lined or filled with aqueous solution, as evidence  
346 suggests (van der Weele et al. 1996), ions could diffuse along the inside of the lacunae and be  
347 taken up by cortical cells. The rate of movement of solutes toward the stele would be much  
348 faster in this case, based on dye diffusion experiments (van der Weele et al. 1996). The  
349 irregularity of occurrence of these water-filled or water-lined lacunae (van der Weele et al.  
350 1996) could account for some of the variability in our nutrient transport data. The generally  
351 negative effects of RCA on nutrient transport in our experiments suggests that the tortuosity

352 imposed by loss of cortical cells was more important than any advantage gained by water  
353 content of the lacunae.

354 RCA slightly reduced calcium transport, but only in larger diameter roots when all genotypes  
355 were included in the analysis (Table 3). For individual genotypes, only RIL 76 showed  
356 significant RCA effects on calcium uptake (Fig. 5). RIL 76 also had the largest plant mass,  
357 RXSA, and LCA and the lowest RCA. Since calcium intracellular homeostasis is  
358 characterized by low calcium concentrations and therefore low potential symplastic fluxes,  
359 most calcium is probably transported in the apoplast until it passes the endodermis (Clarkson  
360 1984; Drew and Fourcy 1986; Halperin et al. 1997), although Cholewa and Peterson (2004)  
361 concluded that radial movement of  $\text{Ca}^{2+}$  in the root occurs at least partially in the symplast. It  
362 is possible that the interruption in apoplastic flow caused by RCA was important only in the  
363 context of larger roots with longer apoplastic pathways. Interestingly, the effect of stele size  
364 on nutrient transport was positive for phosphate and sulfate but negative for calcium.

365 Previous studies reported that RCA does not reduce radial nutrient transport in maize (Drew  
366 and Fourcy 1986), and may even increase it (Drew and Saker 1986; van der Weele et al.  
367 1996). Drew and Saker (1986) measured transport of  $^{32}\text{P}$ ,  $^{86}\text{Rb}$ , and  $^{36}\text{Cl}$  and concluded that  
368 radial transport was just as effective in aerenchymatous roots as in non-aerenchymatous  
369 roots. The movement of both  $\text{Rb}^+$  and  $\text{Sr}^{2+}$  (as analogs of  $\text{K}^+$  and  $\text{Ca}^{2+}$ ) towards the  
370 endodermis in aerenchymatous roots was interpreted by the authors as confirmation that RCA  
371 did not reduce radial nutrient transport. Our results confirm that nutrient uptake is ongoing  
372 across the cortex of aerenchymatous maize roots. However, the previous studies induced  
373 RCA formation using a hypoxic pre-treatment, which may have had additional effects (e.g.  
374 via reduced ATP levels) on subsequent nutrient transport apart from any direct influence of  
375 RCA (e.g. Drew *et al.*, 1980; Drew and Saker, 1986). Low oxygen supply has been shown to  
376 reduce both root hydraulic conductance and ion uptake of maize grown in solution culture,  
377 and these effects were not reversible within 5 h (Birner and Steudle 1993). We observed no  
378 effect or a negative relationship between RCA and nutrient uptake, quantified as transport to  
379 distal tissue, where variation in the amount of RCA was produced by genetic contrasts and  
380 ethylene or 1-MCP treatments. Since ethylene is a part of the normal signal transduction  
381 pathway for aerenchyma formation in maize (Drew et al. 2000), its use as an RCA-inducing  
382 treatment is unlikely to cause artifacts. Therefore, the different conclusions on the effects of  
383 RCA formation on nutrient uptake between previous studies and ours appear to be a  
384 combination of interpretation of results and methodology.

385 Although the genotypes in this study were closely related, significant variation among  
386 genotypes was observed for growth and RCA formation. In experiment 1 using root  
387 segments, genotypes with a greater range of RCA values were used, and the impact of RCA  
388 on  $^{32}\text{P}$  uptake and transport was highly significant. In experiment 2, only RIL 39 showed a  
389 significant effect of RCA on  $^{32}\text{P}$  uptake (Table 3), but of the three genotypes in this study,  
390 this genotype had the highest RCA and the greatest range in RCA values (Table 2). Lateral  
391 root number had a significant effect on phosphate transport in both sets of experiments (Table  
392 3). For the low RCA genotype RIL 321, which had many lateral roots in the  $^{32}\text{P}$  treatment  
393 zone, some replicates had phosphate uptake values that were even higher than the  $I_{\text{max}}$  for  
394 phosphate uptake calculated by (Bhadoria *et al.* 2004). This suggests that lateral roots played  
395 an important role for phosphate uptake, and might be an important route for phosphate  
396 loading from outside the root into the xylem of the seminal root. Further, the lateral roots  
397 increased the root surface area available for phosphate uptake. Our calculations suggest that

398 the additional surface area from these small lateral roots was not sufficient to explain the  
399 large increase in <sup>32</sup>P uptake. More likely, the lack of suberization of endodermal and  
400 hypodermal layers at the nascent root apex (Ma and Peterson 2003; Baxter et al. 2009), and  
401 possibly the disturbance of the cortical tissue caused by emergence of the lateral root (Kumpf  
402 et al. 2013), could have provided high-volume pathways for nutrient uptake. Likewise, root  
403 hairs and root cross-sectional area (RXSA) contributed to <sup>32</sup>P uptake in experiment 2 (Table  
404 3), most likely as a result of the increased surface area for P uptake.

405 In conclusion, we observed slight negative correlations between radial nutrient transport and  
406 RCA formation, and nutrient transport was highly variable due to variation in root attributes  
407 other than RCA. High RCA genotypes had low phosphate uptake based on the time course  
408 study. Additional research is necessary in order to assess potential trade-offs of RCA for  
409 plant productivity, including studies in nutrient-deficient conditions and those measuring  
410 RCA in the entire root system.

#### 411 ACKNOWLEDGEMENTS

412 This research was supported by the USDA NRI Plant Biology Program grant #2007-02001.  
413 We thank Amy Burton, Claire Lorts Kirt, and Larry York for their kind help during  
414 experiment 1 and Robert Snyder for support during experiment 2.

#### 415 LITERATURE CITED

416 **Baxter I, Hosmani PS, Rus A, Lahner B, Borevitz JO, Muthukumar B, Mickelbart M V,**  
417 **Schreiber L, Franke RB, Salt DE. 2009.** Root Suberin Forms an Extracellular Barrier That  
418 Affects Water Relations and Mineral Nutrition in Arabidopsis. *PLoS Genetics* **5**: e1000492.

419 **Bhadoria PS, El Dessougi H, Liebersbach H, Claassen N. 2004.** Phosphorus uptake  
420 kinetics, size of root system and growth of maize and groundnut in solution culture. *Plant &*  
421 *Soil* **262**: 327–336.

422 **Birner T, Steudle E. 1993.** Effects of anaerobic conditions on water and solute relations, and  
423 on active transport in roots of maize (*Zea mays* L.). *Planta* **190**: 474–483.

424 **Bouranis DL, Chorianopoulou SN, Siyiannis VF, Protonotarios VE, Hawkesford MJ.**  
425 **2003.** Aerenchyma formation in roots of maize during sulphate starvation. *Planta* **217**: 382–  
426 391.

427 **Burton AL, Williams MS, Lynch JP, Brown KM. 2012.** RootScan: Software for high-  
428 throughput analysis of root anatomical traits. *Plant & Soil* **357**: 189–203.

429 **Cholewa E, Peterson CA. 2004.** Evidence for Symplastic Involvement in the Radial  
430 Movement of Calcium in Onion Roots. *Plant Physiology* **134**: 1793–1802.

431 **Clarkson DT. 1984.** Calcium transport between tissues and its distribution in the plant. *Plant*  
432 *Cell and Environment* **7**: 449–456.

- 433 **Drew MC, Chamel A, Garrec J-P, Fourcy A. 1980.** Cortical Air Spaces (Aerenchyma) in  
434 Roots of Corn Subjected to Oxygen Stress: Structure and influence on uptake and  
435 translocation of 86rubidium ions. *Plant Physiology* **65**: 506–511.
- 436 **Drew MC, Fourcy A. 1986.** Radial Movement of Cations across Aerenchymatous Roots of  
437 *Zea mays* Measured by Electron Probe X-Ray Microanalysis. *Journal of Experimental*  
438 *Botany* **37**: 823–831.
- 439 **Drew MC, He C jiu, Morgan PW. 2000.** Programmed cell death and aerenchyma formation  
440 in roots. *Trends in Plant Science* **5**: 123–127.
- 441 **Drew MC, Saker LR. 1986.** Ion transport to the xylem in aerenchymatous roots of *Zea mays*  
442 *L.* *Journal of Experimental Botany* **37**: 22–33.
- 443 **Esau K. 1977.** *Anatomy of seed plants*. New York, New York: John Wiley and Sons.
- 444 **Evans DE. 2003.** Aerenchyma formation. *New Phytologist* **161**: 35–49.
- 445 **Fan MS, Bai RQ, Zhao XF, Zhang JH. 2007.** Aerenchyma formed under phosphorus  
446 deficiency contributes to the reduced root hydraulic conductivity in maize roots. *Journal of*  
447 *Integrative Plant Biology* **49**: 598–604.
- 448 **Fan MS, Zhu JM, Richards C, Brown KM, Lynch JP. 2003.** Physiological roles for  
449 aerenchyma in phosphorus-stressed roots. *Functional Plant Biology* **30**: 493–506.
- 450 **Gunawardena AHLAN, Pearce DM, Jackson MB, Hawes CR, Evans DE. 2001.**  
451 Characterisation of programmed cell death during aerenchyma formation induced by ethylene  
452 or hypoxia in roots of maize (*Zea mays* L.). *Planta* **212**: 205–214.
- 453 **Halperin SJ, Kochian L V, Lynch JP. 1997.** Salinity stress inhibits calcium loading into the  
454 xylem of excised barley (*Hordeum vulgare*) roots. *New Phytologist* **135**: 419–427.
- 455 **He C jiu, Morgan PW, Drew MC. 1996.** Transduction of an ethylene signal is required for  
456 cell death and lysis in the root cortex of maize during aerenchyma formation induced by  
457 hypoxia. *Plant Physiology* **112**: 463–472.
- 458 **Kumpf RP, Shi C-L, Larrieu A, Stø IM, Butenko MA, Péret B, Riiser ES, Bennett MJ,**  
459 **Aalen RB. 2013.** Floral organ abscission peptide IDA and its HAE/HSL2 receptors control  
460 cell separation during lateral root emergence. *Proceedings of the National Academy of*  
461 *Sciences USA* **110**: 5235–5240.
- 462 **Lynch JP, Brown KM. 1998.** Root Architecture and Phosphorus Acquisition Efficiency in  
463 Common Bean. In: Lynch J P, Deikman J, eds. *Phosphorus in Plant Biology: Regulatory*  
464 *Roles in Ecosystem, Organismic, Cellular, and Molecular Processes*. Rockville, MD: ASPP,  
465 148–156.
- 466 **Lynch JP, Läuchli A. 1984.** Potassium transport in salt-stressed barley roots. *Planta* **161**:  
467 295–301.

- 468 **Ma F, Peterson CA. 2003.** Current insights into the development, structure, and chemistry of  
469 the endodermis and exodermis of roots. *Canadian Journal of Botany* **421**: 405–421.
- 470 **Naeve SL, Shibles RM. 2005.** Distribution and mobilization of sulfur during soybean  
471 reproduction. *Crop Science* **45**: 2540–2551.
- 472 **Postma JA, Lynch JP. 2010.** Theoretical evidence for the functional benefit of root cortical  
473 aerenchyma in soils with low phosphorus availability. *Annals of Botany*.
- 474 **Postma JA, Lynch JP. 2011.** Root cortical aerenchyma enhances the growth of maize on  
475 soils with suboptimal availability of nitrogen, phosphorus, and potassium. *Plant Physiology*  
476 **156**: 1190–1201.
- 477 **Striker GG, Insausti P, Grimoldi AA, Vega AS. 2007.** Trade-off between root porosity and  
478 mechanical strength in species with different types of aerenchyma. *Plant Cell and*  
479 *Environment* **30**: 580–589.
- 480 **Tester M, Leigh R. 2001.** Partitioning of nutrient transport processes in roots. *Journal of*  
481 *Experimental Botany* **52**: 445–57.
- 482 **Van der Weele CM, Canny MJ, McCully ME. 1996.** Water in aerenchyma spaces in roots.  
483 A fast diffusion path for solutes. *Plant & Soil* **V184**: 131–141.
- 484 **Zhu JM, Brown KM, Lynch JP. 2010.** Root cortical aerenchyma improves the drought  
485 tolerance of maize (*Zea mays* L.). *Plant Cell and Environment* **33**: 740–749.
- 486
- 487

488

## 489 Figure legends

490

491 Fig. 1. Experimental setups for radionuclide application to root segments. A. For experiment  
492 1, a modified Pitman chamber was used to treat a 7.4 mm. segment of an excised first-whorl  
493 crown root. This top view of the plexiglass chamber shows the 0.5 ml receiver compartment,  
494 where  $^{32}\text{P}$  exudation from the cut end of the root was measured, the 1 ml treatment chamber  
495 where the  $^{32}\text{P}$  was added, and the 1 ml leakage check compartment adjacent to the treatment  
496 compartment. The root tip was in a water bath containing unlabeled nutrient solution. P  
497 uptake was measured by adding the counts from the receiver compartment and those from  
498 the root segment therein. B. The chamber for experiment 2 permitted application of labeled  
499 nutrients to a 6 mm region of an intact maize seminal root. A 100 ml cup contained the  
500 whole plant, with the roots bathing in nutrient solution. One seminal root was inserted  
501 through two holes in a polypropylene tube, the openings sealed with silicon grease, and  
502 radionuclide solution added to the tube.

503

504 Fig. 2. Cross-sections from radionuclide-treated root segments from each genotype used in  
505 this study showing root cortical aerenchyma (RCA) formation. Images shown are  
506 representative of average RCA values for each treatment. The six images on the left are  
507 from experiment 1, where each side-by-side pair was studied at the same time, and the six  
508 images on the right from experiment 2, where each of the three treatments were compared at  
509 the same time. The size bar in each image represents 400  $\mu\text{m}$ .

510

511 Fig. 3. Negative relationship between  $^{32}\text{P}$  uptake and % RCA in six maize genotypes in  
512 experiment 1. The effect is significant at  $P < 0.0001$ .

513

514 Fig. 4. Time course of cumulative  $^{32}\text{P}$  exudation in three high RCA genotypes (closed  
515 symbols) and three low RCA genotypes (open symbols) in experiment 1. Error bars  
516 represent SE. RIL 360 is not visible because it is directly behind RIL 345.

517 Fig. 5. Direct relationships between nutrient uptake and RCA in segments of intact maize  
518 seminal roots in experiment 2. A) Calcium transport was negatively correlated with RCA  
519 formation in RIL 76 ( $r^2=0.337$ ,  $P=0.029$ ,  $y=0.359-2.87x$ ). B) Phosphate transport was  
520 negatively correlated with RCA formation in RIL 364 ( $r^2=0.388$ ,  $P=0.017$ ,  $y=2.59-0.923x$ ).  
521 C) A decreasing trend in sulfur transport was observed in RIL 39, although this was not  
522 significant ( $r^2=0.099$ ,  $P=0.204$ ).

523 **Table 1.** Root anatomical traits and <sup>32</sup>P uptake rates of 7.4 mm root segments of 6 maize RILs grown in hydroponics  
524 for 12 days in experiment 1. Values shown are means ± standard error for root cross sectional area (RXSA), stele area  
525 (SA), percent root cortical aerenchyma area (%RCA), and lateral root number (LRN). The RCA categories show the  
526 paired comparisons for simultaneous measurements. Means within columns followed by the same letter are not  
527 significantly different according to Tukey's test at P<0.05.

	RCA category	RXSA (mm <sup>2</sup> )	SA (mm <sup>2</sup> )	%RCA	LRN (per <sup>32</sup> P treated segment)	P uptake pmol mm <sup>-2</sup> h <sup>-1</sup>
RIL 369	low	1.77 ± 0.22 a	0.25 ± 0.06 ab	0.76 ± 0.58 c	2.17 ± 0.98 b	3.838 ± 0.687 c
RIL 15	high	1.37 ± 0.08 b	0.22 ± 0.02 b	10.24 ± 1.11 a	0.75 ± 0.50 c	0.386 ± 0.053 d
RIL 321	low	1.38 ± 0.14 b	0.28 ± 0.04 a	2.01 ± 0.74 c	7.67 ± 1.51 a	11.118 ± 0.403 a
RIL 360	high	0.91 ± 0.20 c	0.17 ± 0.05 c	6.14 ± 1.68 b	0.67 ± 1.21 c	4.288 ± 0.461 c
RIL 61	low	1.89 ± 0.46 a	0.29 ± 0.04 a	1.56 ± 0.52 c	0.38 ± 0.74 c	6.074 ± 1.202 b
RIL 345	high	1.32 ± 0.18 b	0.22 ± 0.02 b	6.97 ± 1.52 b	0.63 ± 0.74 c	3.978 ± 0.493 c

528

529

530





532 **Table 2.** Plant growth and root traits in maize RILs grown in solution culture with root-zone ethylene and  
 533 1-MCP (1-methylcyclopropene) treatments in experiment 2. Significant differences among treatments of a  
 534 given genotype as determined by one-way ANOVA are denoted by different letters. Cases where RCA  
 535 formation in the 1-MCP treatment was determined to be significantly lower than the ethylene treatment by t-  
 536 test are denoted by \*. Values shown are means  $\pm$  standard error, and n= 18 in each case

	Plant dry mass (g)	RXSA <sup>a</sup> (mm <sup>2</sup> )	SA <sup>b</sup> (% of RXSA)	LRN <sup>c</sup> (# per 6-mm root segment)	Root hair rating (0-5)	%RCA <sup>d</sup>	LCA <sup>e</sup> (mm <sup>2</sup> )
RIL 39 control	0.13 $\pm$ 0.02	1.49 $\pm$ 0.11a	14.93 $\pm$ 0.28a	3.33 $\pm$ 0.55	0.22 $\pm$ 0.19	8.15 $\pm$ 1.75	1.16 $\pm$ 0.09
RIL 39 ethylene	0.13 $\pm$ 0.02	1.59 $\pm$ 0.08a	15.49 $\pm$ 0.56a	2.72 $\pm$ 0.56	0.26 $\pm$ 0.13	8.65 $\pm$ 1.36	1.24 $\pm$ 0.08
RIL 39 1-MCP	0.13 $\pm$ 0.02	1.10 $\pm$ 0.12b	18.14 $\pm$ 0.44b	3.06 $\pm$ 0.60	0.02 $\pm$ 0.02	11.34 $\pm$ 1.30	0.79 $\pm$ 0.09
RIL 76 control	0.33 $\pm$ 0.03	2.03 $\pm$ 0.09	16.37 $\pm$ 0.59	7.78 $\pm$ 0.91a	1.12 $\pm$ 0.29	3.25 $\pm$ 1.14	1.65 $\pm$ 0.09
RIL 76 ethylene	0.29 $\pm$ 0.03	1.90 $\pm$ 0.12	15.70 $\pm$ 0.58	4.78 $\pm$ 1.01b	0.93 $\pm$ 0.31	3.65 $\pm$ 0.90	1.54 $\pm$ 0.10
RIL 76 1-MCP	0.31 $\pm$ 0.04	1.73 $\pm$ 0.18	16.78 $\pm$ 0.71	4.11 $\pm$ 0.72c	0.92 $\pm$ 0.32	1.31 $\pm$ 0.63*	1.43 $\pm$ 0.16
RIL 364 control	0.17 $\pm$ 0.01	1.37 $\pm$ 0.11	15.47 $\pm$ 0.44	4.17 $\pm$ 0.35	1.20 $\pm$ 0.27	3.43 $\pm$ 0.84	1.11 $\pm$ 0.09
RIL 364 ethylene	0.17 $\pm$ 0.02	1.41 $\pm$ 0.09	15.57 $\pm$ 0.42	3.72 $\pm$ 0.65	0.86 $\pm$ 0.24	5.44 $\pm$ 1.19	1.13 $\pm$ 0.08
RIL 364 1-MCP	0.16 $\pm$ 0.01	1.61 $\pm$ 0.11	15.39 $\pm$ 0.55	4.00 $\pm$ 0.68	1.49 $\pm$ 0.22	3.17 $\pm$ 0.81*	1.32 $\pm$ 0.09

537 <sup>a</sup> RXSA = root cross sectional area; <sup>b</sup>: SA – stele area as percent of RXSA; <sup>c</sup> LRN = lateral root number; <sup>d</sup> RCA area as percent of  
 538 cortical area; <sup>e</sup> LCA = living cortical area, calculated as total cortical area – RCA area.

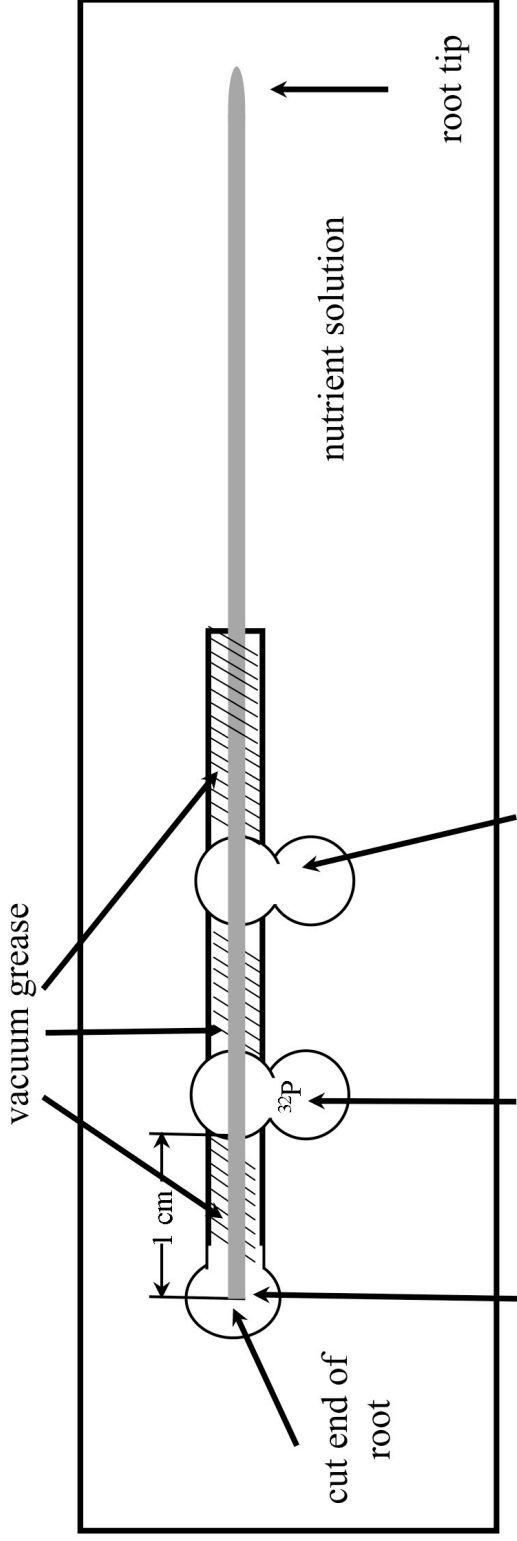
539

540  
541  
542  
543  
544  
545

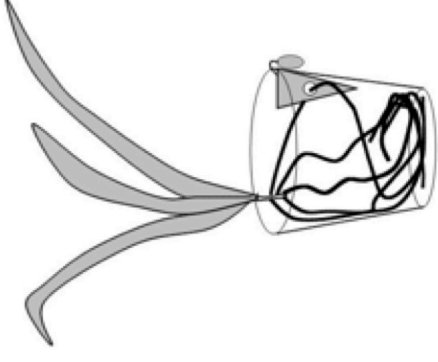
**Table 3.** Multiple regression models for root anatomical traits that affected nutrient transport in experiment 2. For each nutrient, the sample groups are listed for which a significant regression model was identified, as well as the root traits in the model, their significance levels, and the overall fit ( $r^2$ ) of the model.

Nutrient	Sample group	Dependent variables (y)	Independent variables	Sign.	Regression Equation	$r^2$
calcium	RXSA > 1.5 mm <sup>2</sup>	log uptake (nmol)	model	0.006	y = 0.047 - 2.14 x 10 <sup>-4</sup> a -0.006b	0.416
			a %SA	0.005		
			b log %RCA	0.074		
	RIL 364	log uptake (nmol g <sup>-1</sup> )	a LRN	0.018	y = 0.386-0.006a	0.412
phosphorus	RIL 39	log uptake (nmol g <sup>-1</sup> )	model	0.006	y = -1.091 + 0.232a - 1.001.041b - 0.416c - 0.366d - 0.008e	1.00
			a %SA	0.006		
			b log %RCA	0.008		
			c root hair rating	0.010		
			d RXSA (mm <sup>2</sup> )	0.009		
			e LRN	0.007		
sulfur	RXSA = 0.5- 1.5 mm <sup>2</sup>	log uptake (nmol)	a LRN	0.004	y = 0.963 + 0.096a	0.327
	RXSA > 1.5 mm <sup>2</sup>	log uptake (nmol)	a %SA	0.077	y = 1.093 + 0.036a	0.125

A

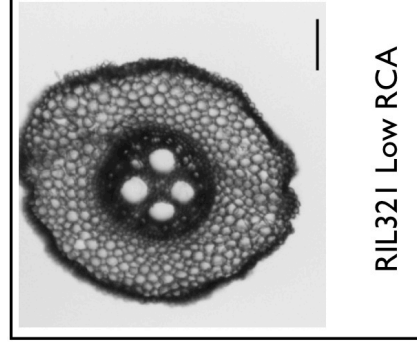
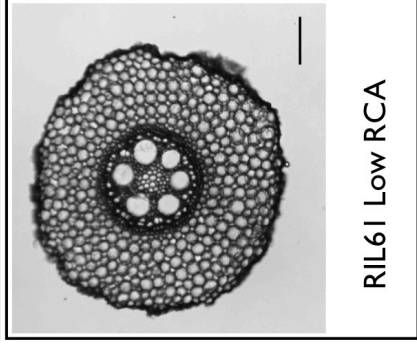
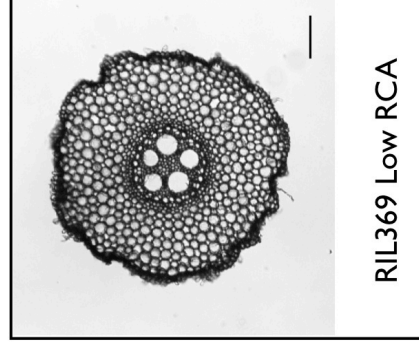
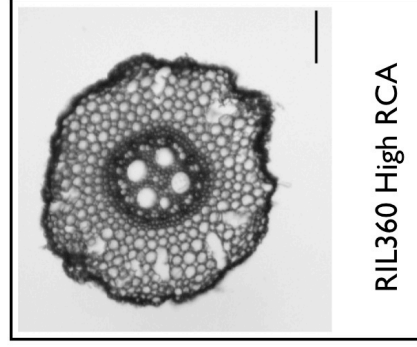
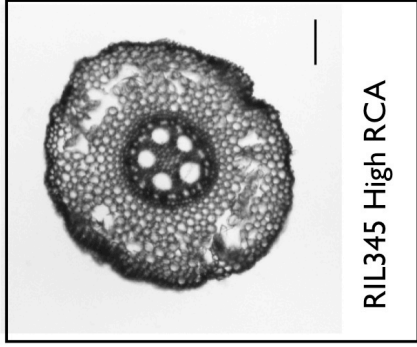
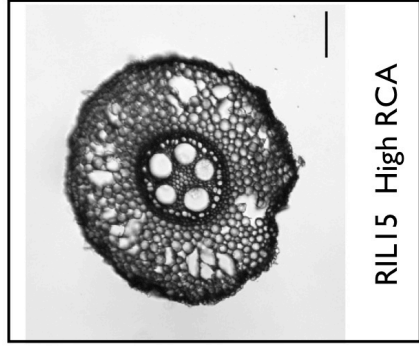


B



0.5 ml receiver compartment    1 ml treatment compartment    1 ml leakage check compartment

Experiment 1



Experiment 2

